

# Catalyst-Free Growth of GaN Nanowires

K.A. BERTNESS,<sup>1,3</sup> N.A. SANFORD,<sup>1</sup> J.M. BARKER,<sup>1</sup> J.B. SCHLAGER,<sup>1</sup>  
A. ROSHKO,<sup>1</sup> A.V. DAVYDOV,<sup>2</sup> and I. LEVIN<sup>2</sup>

1.—National Institute of Standards and Technology, Boulder, CO 80305. 2.—National Institute of Standards and Technology, Gaithersburg, MD 20899-8555. 3.—E-mail: bertness@boulder.nist.gov

We have grown GaN and AlGaInN nanowires on Si (111) substrates with gas-source molecular beam epitaxy (MBE). No metal catalysts were used. The nanowires displayed a number of interesting materials properties, including room-temperature luminescence intensity greater than that of free-standing HVPE-grown GaN, relaxed lattice parameters, and the tendency of nanowires dispersed in solvents to align in response to electric fields. The wires were well separated, 50–250 nm in diameter, and grew to lengths ranging from 2  $\mu\text{m}$  to 7  $\mu\text{m}$ . Transmission electron microscopy indicated that the wires were free of defects, unlike the surrounding matrix layer.

**Key words:** Gallium nitride, molecular beam epitaxy (MBE), nanostructures, nanotechnology

## INTRODUCTION

The growth of semiconductors in nanowire structures has increased dramatically upon the identification of catalytic methods for preferential growth along a single axis. The catalysts are typically droplets of gold, nickel, or other metals, and growth under the droplet proceeds by means of the vapor-liquid-solid (VLS) mechanism. The details of the mechanism are still under study;<sup>1</sup> however, the progress in terms of device demonstration has been remarkable. The nanowire growth regime is particularly attractive for the AlGaInN alloy system, because lattice-matched substrates for this system are not readily available. The nanowire morphology also allows greater dislocation-free strain relaxation in response to heterojunction formation and cooling after crystal growth. GaN nanowire lasers,<sup>2</sup> light-emitting diodes,<sup>3,4</sup> and transistors<sup>5</sup> are among early technological demonstrations emerging from these structures. Like any growth method, however, catalytic growth does have some limitations. Growth conditions are limited to temperature ranges compatible with the catalyst, and preparation of the catalyst dots requires additional steps. The question of the effect on luminescent efficiency of impurity-level incorporation of the metals into the semiconductor has not yet been addressed quantitatively.

For this reason, some applications may require the use of catalyst-free growth methods. Noncatalytic growth of nanowires has been reported by only a handful of groups,<sup>6–10</sup> including those groups using GaN seed crystal methods to nucleate nanowires.

In this paper, we discuss growth conditions for catalyst-free growth of GaN and AlGaInN nanowires on Si substrates using molecular beam epitaxy (MBE) and present data illustrating some of the interesting nanowire properties. We observed indications of very high material quality, including high intensity of photoluminescence (PL) at room temperature, relaxed lattice parameters, and absence of structural defects as observed by transmission electron microscopy (TEM). The wires also exhibited a tendency to align in response to external electric fields, and this property has been used to assist in the placement of wires dispersed in solvents onto metal contact pads.

## EXPERIMENTAL PROCEDURES

The nanowire growths took place in a conventional gas-source MBE system with evaporator cells for Ga, Al, Si, and Be and an radio-frequency plasma N source. The operating conditions during growth of GaN nanowires were a nitrogen flow of 2.1  $\mu\text{mol/s}$  (3 sccm), with 450 W of RF power for the nitrogen source, and a Ga beam equivalent pressure of  $1.3 \times 10^{-5}$  Pa. Substrate temperatures were measured

with an optical pyrometer, which yielded measurements with an expanded uncertainty of approximately 8°C. Si (111) wafers were prepared for growth by etching in a 10% HF:H<sub>2</sub>O mixture by volume, rinsing with deionized water, and blowing dry. The substrates were outgassed in a preparation chamber at 750°C ± 15°C for 15 min., and then outgassed again at 850°C for 10 min. in the growth chamber. Growth was initiated with a 0.5-nm layer of pure Al at 700°C, followed by 50–80 nm of AlN at a growth temperature of 630°C. The nanowires were typically grown at a substrate temperature of 820°C. Further details of the growth conditions and responses to variations in nitrogen and Ga flux are being published separately.<sup>11</sup>

## RESULTS AND DISCUSSION

Typical GaN nanowire morphology is illustrated in Fig. 1. The wires were well separated with hexagonal cross section, 50–150 nm in diameter and extending about 2 μm above the matrix layer in this sample. Although the wire diameters varied by a factor of 3, the wire lengths were within about 15% of one another. Because wires maintained their diameter as they grew, the wire diameter was most likely determined during the nucleation process. As can be seen in Fig. 1, the sidewalls of the nanowires were aligned to one another, and x-ray diffraction

revealed that the GaN  $\langle 11\bar{2}0 \rangle$  directions were aligned with the Si  $\langle 1\bar{1}0 \rangle$  directions.<sup>12</sup> This crystal registration was the same as that observed for thin film growth of GaN on Si. Comparison of the sidewalls with the flat on the Si wafer confirmed that the sidewalls conform to GaN  $\{10\bar{1}0\}$  planes. The wires grew out of an irregularly faceted matrix layer and, generally, but not always, appeared to nucleate deep within the matrix.

As shown in Table I, despite the large mismatch in lattice parameter and in thermal expansion coefficients between Si and GaN, the nanowires were nearly relaxed to bulk GaN values.<sup>13</sup> Perhaps more surprising is that the matrix layers were mostly relaxed and only slightly broader, as illustrated in Fig. 2 and Table I. The rocking curve widths for these peaks were also small, 0.3–0.8°, indicating that the nanowires were quite straight and that the matrix was highly aligned. The nanowire (0002) x-ray diffraction was narrower and mostly disappeared when the wire sections above the matrix were removed by polishing. For thicker specimens, the contributions of the nanowires and matrix could not always be entirely distinguished in the x-ray diffraction. In addition to the structures visible in Fig. 1, larger structures that we call “fins” grew tilted relative to the surface, often occurring in pairs to form a v-shape. We have not yet identified the orientation of these structures.

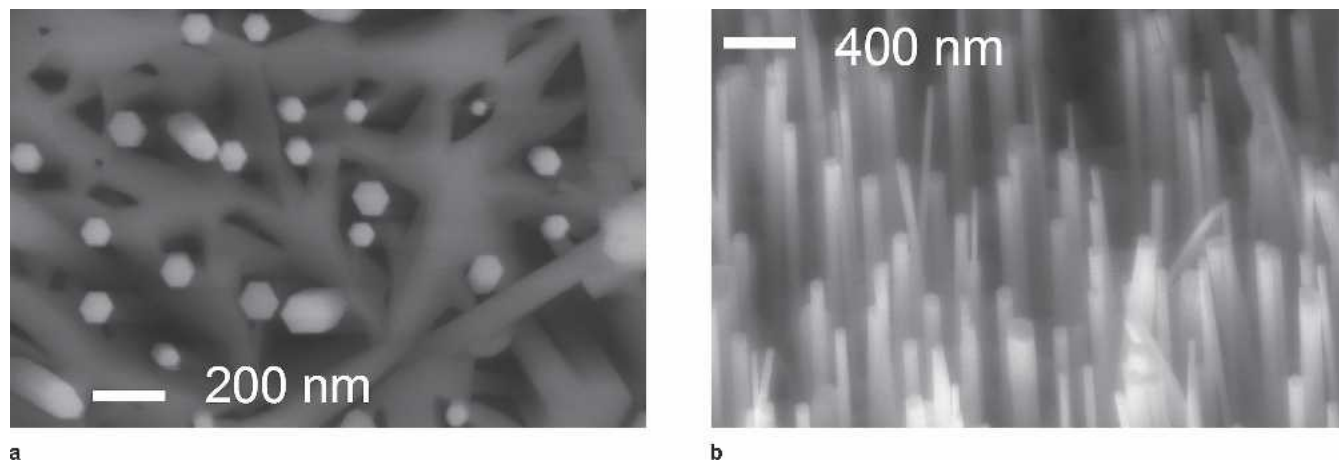


Fig. 1. Field-emission scanning electron microscopy image of GaN nanowires (a) in plan view and (b) viewed 30° from specimen normal. The faceted matrix is also visible in the top view.

Table I. Lattice Parameters for Nanowire Specimens and the Matrix Layer, Compared with Bulk GaN (Ref.13)\*

Lattice Parameter	Wires c	Wires a	Matrix c
B724, 3 μm nanowires	0.518 53 ± 0.000 05	0.318 93 ± 0.000 10	0.518 33 ± 0.000 08
B738, 6 μm nanowires	0.518 46 ± 0.000 04	0.318 98 ± 0.000 10	(Indistinguishable from nanowires)
Bulk undoped	0.518 46	0.318 76	—

\*The uncertainties given are expanded to twice the standard deviation for 95% confidence interval and include both spatial variations in the specimens as well as instrument precision.

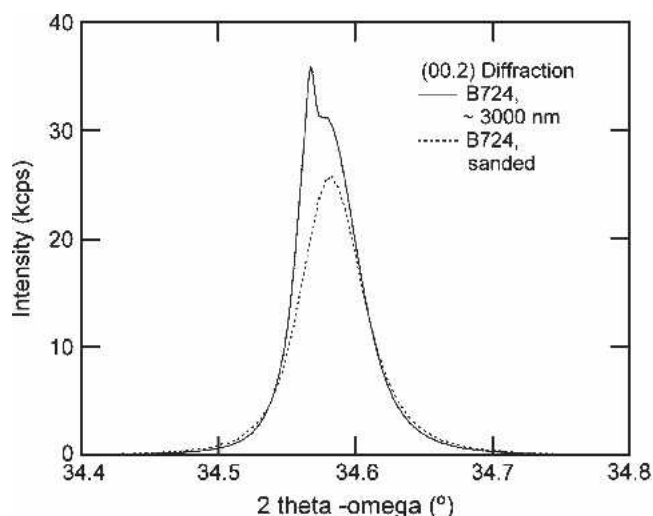


Fig. 2. X-ray diffraction 2 theta-omega scan over the (0002) diffraction peak for a GaN nanowire specimen and the same specimen after the wire tops and some of the matrix were removed by polishing.

Although the nanowires and matrix material had similar lattice constants, their defect structure was quite different. The TEM images in Fig. 3 show that the nanowires were free of visible defects, while the

matrix structures had a high density of basal plane stacking faults. These faults generated streaking along the [0001] direction in the TEM diffraction patterns (not shown). The high degree of crystalline perfection in the nanowires was also demonstrated in room-temperature PL taken with excitation at 325 nm (3.81 eV). The peak PL intensity (Fig. 4) for the nanowire as-grown specimen is almost twice the intensity observed for a free-standing HVPE GaN platelet examined under the same excitation and collection conditions, despite the smaller effective volume of the nanowire specimen. The high quality of the HVPE GaN platelet<sup>14</sup> is demonstrated by its low rocking curve widths of 0.024° and 0.032°, respectively, for the (0006) and (0004) x-ray diffraction peaks and strong phonon replica peaks in the low-temperature PL spectrum (not shown). We also have evidence that the luminescence from the GaN matrix layer had greater contributions from below-gap defect states than did the nanowires. Specifically, in low-temperature PL data, specimens with nanowires removed through rough polishing produced lower luminescence intensity at the donor-bound exciton peak at 3.472 eV, and a much higher intensity of below-gap emission, relative to as-grown specimens with the nanowires fully intact.

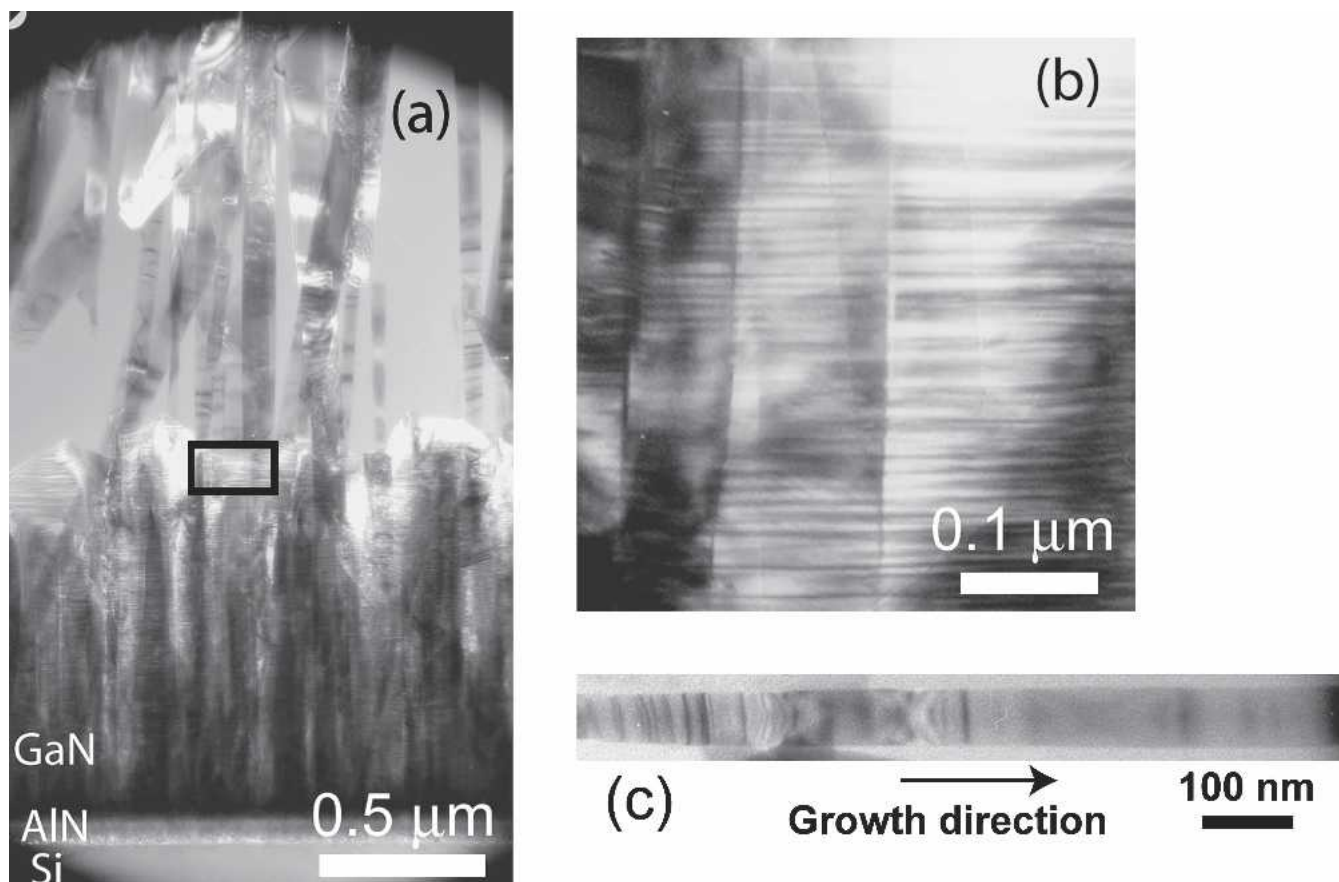


Fig. 3. TEM images of GaN nanowires and matrix layers. The rectangle in (a) is expanded for greater clarity in (b), showing how the tops of the matrix layer peaks contained a high density of basal plane stacking faults. A dark-field image of a single, typical GaN nanowire is given in (c). The bandlike contrast seen in nanowire images (a) and (c) is associated with the nanowire bending. No contrast characteristic of extended defects (i.e., dislocations, stacking faults, etc.) was observed.

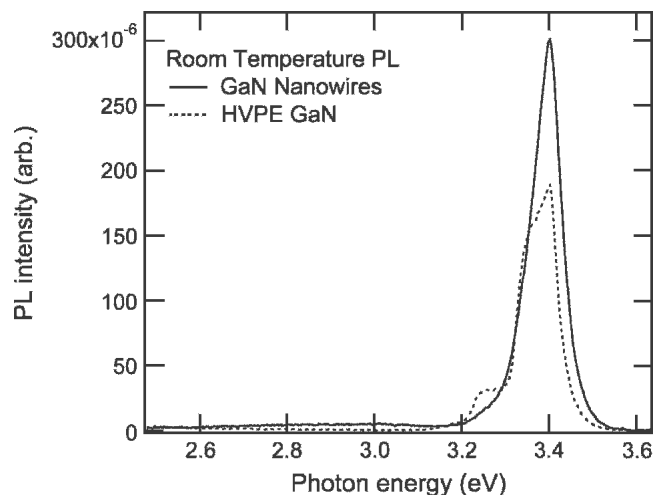


Fig. 4. Room-temperature PL on GaN nanowires, illustrating that the luminescent intensity is higher than the intensity from a free-standing, high-quality HVPE GaN film measured under the same excitation conditions.

For both device applications and materials characterization, it is useful to remove the nanowires from the growth substrate. This removal was possible with the simple procedure of placing a piece of as-grown wafer in a solvent (acetone, hexane, etc.) and agitating the mixture in an ultrasonic bath. The liquid containing nanowires was transferred with pipettes to new substrates, and upon evaporation of the solvent, the wires remained behind. Nanowires transferred in this way adhered through subsequent processing steps (photolithography, etc.), although they could be removed with intentional scrubbing. We observed that wires preferred to adhere to metal pads or oriented perpendicular to the edges of pads when the pads were on an insulating substrate such as sapphire. Over 90% of short wires (2.5  $\mu\text{m}$ ) behaved in this way. Similar behavior occurred with longer wires (6  $\mu\text{m}$ ), but these nanowires required application of a voltage between metal patterns during dispersal to display alignment. An example of nanowires dispersed with the assistance of electric fields is given in the SEM picture in Fig. 5. Not unexpectedly, the effect was observed only in nonpolar solvents (hexane and toluene); because of their relatively higher dielectric constants, polar solvents such as water, methanol, and acetone were less effective at facilitating alignment.

The mechanism for the growth of the GaN nanowires is still unclear. Although previous workers with similar results have postulated a VLS growth mechanism<sup>15</sup> with Ga droplets serving as the catalyst, neither they nor we have ever observed droplets remaining on the tips of the nanowires. After completion of growth, and the removal of the samples from the growth chamber, the wires tips tended to be sharply faceted. AlGaIn nanowires, in particular, frequently terminated in planes tilted relative to the growth axis. The Ga droplets are known to form under Ga-rich conditions during MBE growth,

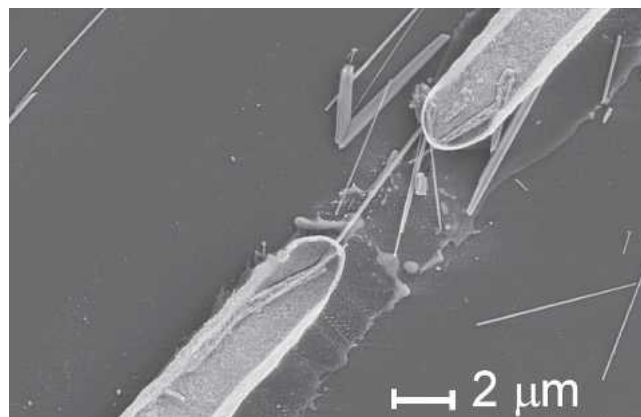


Fig. 5. GaN nanowires aligned to two metal pads. Stray wires are also present on the surface as well as solvent residue. A v-shaped fin structure was deposited on the left of the upper pad.

but under the N-rich conditions that promote nanowire growth, any excess Ga is expected to be rapidly incorporated into the crystal. Furthermore, we have observed<sup>11</sup> that changing the growth conditions in a way that would be expected to alter surface diffusion of the group III atoms alters the overall growth morphology substantially. Specifically, the addition of Be, a known surfactant that stimulates surface diffusion, transforms the entire morphology into vertical ribbons that tend to align with the low-energy  $\{10\bar{1}0\}$  planes. In contrast, the addition of Al for the growth of AlGaIn wires slows the surface diffusion. AlGaIn wires nucleate with relatively small diameters but subsequently increase in diameter as the growth progresses under the same temperature and V:III flux ratios, whereas GaN nanowires grow with uniform diameter indefinitely. While much remains to be confirmed about the mechanism, we tentatively conclude that differences in surface diffusion (or, conversely, surface sticking coefficient) are a major if not the only driving force for the formation of the wires in MBE. Nanowire formation is therefore a kinetic phenomenon, depending on the detailed balance between different diffusion and incorporation processes.

## SUMMARY

We have demonstrated growth of GaN and AlGaIn nanowires with high aspect ratio on Si (111) substrates using MBE. The wires had high luminescent efficiency at room temperature compared with that of free-standing GaN platelets and appeared to be free of structural defects in TEM. Despite the large mismatch between the Si substrate and GaN, the lattice parameters for the wires were essentially the same as for bulk GaN. The growth mechanism for the wires appears to differ from that which drives catalytic growth of nanowires in vapor-phase methods, although both mechanisms may depend in part on the stability of the nonpolar  $\{10\bar{1}0\}$  GaN planes. The wires were readily transferred from the growth substrate to alternative substrates through ultrasonic agitation in solvents. The orientation and

placement of wires onto substrates from suspension in nonpolar solvents could be facilitated by the application of electric fields.

### ACKNOWLEDGEMENTS

The paper is a contribution of an agency of the United States government and is not subject to copyright. We gratefully acknowledge David Look and Colin Wood for assistance in obtaining the free-standing HVPE GaN material.

### REFERENCES

1. W. Seifert et al., *J. Cryst. Growth* 272, 211 (2004).
2. J.C. Johnson, H.-J. Choi, K.P. Knutsen, R.D. Schaller, P. Yang, and R.J. Saykally, *Nat. Mater.* 1, 106 (2002).
3. Z. Zhong, F. Qian, D. Wang, and C.M. Lieber, *Nano Lett.* 3, 343 (2003).
4. F. Qian, Y. Li, S. Gradecjak, D. Wang, C.J. Barrelet, and C.M. Lieber, *Nano Lett.* 4, 1975 (2004).
5. M.C. McAlpine, R.S. Friedman, S. Jin, K.-H. Lin, W.U. Wang, and C.M. Lieber, *Nano Lett.* 3, 1531 (2003).
6. J. Ristic, M.A. Sanchez-Garcia, E. Calleja, J. Sanchez-Paramo, J.M. Calleja, U. Jahn, and K.H. Ploog, *Phys. Status Solidi A-Appl. Res.* 192, 60 (2002).
7. Y.H. Kim, J.Y. Lee, S.-H. Lee, J.-E. Oh, and H.S. Lee, *Appl. Phys. A: Mater. Sci. Process* 80, 1635 (2005).
8. M. Yoshizawa, A. Kikuchi, M. Mori, N. Fujita, and K. Kishino, *Jpn. J. Appl. Phys. Part 2* 36, L459-62 (1997).
9. A. Kikuchi, M. Kawai, M. Tada, and K. Kishino, *Jpn. J. Appl. Phys. Part 2* 43, L1524-26 (2004).
10. R. Calarco, M. Marso, T. Richter, A.I. Aykanat, R. Meijers, A.V. Hart, T. Stoica, and H. Luth, *Nano Lett.* 5, 981 (2005).
11. K.A. Bertness, A. Roshko, N.A. Sanford, J.M. Barker, and A.V. Davydov, *J. Cryst. Growth* 287, 522 (2006).
12. R. Liu, F.A. Ponce, A. Dadgar, and A. Krost, *Appl. Phys. Lett.* 83, 860 (2003).
13. S. Porowski, *J. Cryst. Growth* 190, 153 (1998).
14. S. S. Park, I.-W. Park, and S. H. Choh, *Jpn. J. Appl. Phys. Part 2* 39, L1141-42 (2000).
15. E. Calleja, M.A. Sánchez-García, F.J. Sánchez, F. Calle, F.B. Naranjo, E. Muñoz, U. Jahn, and K. Ploog, *Phys. Rev. B: Condens. Matter Mater. Phys.* 62, 16826 (2000).